Journal of Applied Physics

RESEARCH ARTICLE | DECEMBER 05 2025

Defect analysis of Sn-doped Ga_2O_3/SiC hetero-structured Schottky diodes using deep level transient spectroscopy

Tae-Hee Lee ; Ji-Soo Choi ; Se-Rim Park ; Seung-Hwan Chung ; Geon-Hee Lee ; Jae Hyeok Lim ; Si-Young Bae ; Sang-Mo Koo

J. Appl. Phys. 138, 215703 (2025)
https://doi.org/10.1063/5.0287493

AIP Publishing

Journal of Applied Physics ARTICLE pubs.aip.org/aip/jap

Defect analysis of Sn-doped Ga_2O_3/SiC hetero-structured Schottky diodes using deep level transient spectroscopy

Cite as: J. Appl. Phys. **138**, 215703 (2025); doi: 10.1063/5.0287493
Submitted: 25 June 2025 · Accepted: 27 October 2025 ·
Published Online: 5 December 2025

Tae-Hee Lee,[1] Ji-Soo Choi,[1] Se-Rim Park,[1] Seung-Hwan Chung,[1] Geon-Hee Lee,[1] Jae Hyeok Lim,[2] Si-Young Bae,[3] and Sang-Mo Koo[1,a)]

AFFILIATIONS

[1]Department of Electronic Materials Engineering, Kwangwoon University, Seoul, Republic of Korea
[2]Korea Institute of Ceramic Engineering and Technology, Jinju 52851, Republic of Korea
[3]Department of Nanotechnology and Semiconductor Engineering, Pukyong National University, Pusan, Republic of Korea

[a)]**Author to whom correspondence should be addressed:** smkoo@kw.ac.kr

ABSTRACT

The Sn-doped β-Ga_2O_3 films were fabricated on n-type 4H-SiC substrates using Mist-chemical vapor deposition with different [Sn]/[Ga] ratios of 0%, 3%, 5%, and 10%. For device fabrication, Ni Schottky contacts were deposited on the Ga_2O_3 epilayer by electron-beam evaporation, forming Ga_2O_3/SiC hetero-structured Schottky barrier diodes. The deposition influence on the chemical state, electrical properties, and deep-level traps of Sn-doped Ga_2O_3 films were thoroughly investigated. In J–V characteristics, the Ga_2O_3 film with 3% [Sn]/[Ga] ratio showed the highest conducting properties and lowest $R_{on,sp}$ and leakage current. The results of x-ray photoelectron spectroscopy demonstrated that Sn atoms were successfully doped in these films, and the formation of SnO and SnO_2 could be inferred based on the [Sn]/[Ga] ratio. Deep-level transient spectroscopy (DLTS) identified the $Z_{1/2}$ center (carbon vacancy, V_C) in 4H-SiC for the undoped device and for the SiC epitaxial sample. In Sn-doped devices, Sn-related levels (Sn_{Ga}) were observed, and the $Z_{1/2}$ signal was not detected within our measurement sensitivity. In addition, at higher Sn concentrations, V_O-related defects were detected, which could degrade the leakage current and carrier lifetime. This study provides a pathway to optimize the fabrication of high-performance Sn-doped Ga_2O_3/SiC heterojunction diodes with minimized defect density and enhanced electrical properties.

I. INTRODUCTION

Beta-phase gallium oxide (β-Ga_2O_3) has emerged as a promising ultrawide bandgap semiconductor with a bandgap of approximately 4.62 eV.[1,2] Due to its high breakdown voltage and low on-resistance, β-Ga_2O_3 has attracted significant interest for applications in power electronics and optoelectronic devices, including electric vehicles and renewable energy systems.[3,4]

To fully exploit its potential in high-power and high-frequency applications, precise control of defects and dopants is essential. Deep-level defects critically influence electrical and optical performance by affecting carrier lifetime through non-radiative recombination and introducing challenges such as carrier trapping, compensation, and scattering.[5–7] Among various doping strategies, Sn doping is particularly advantageous due to its impact on both lattice stability and electrical properties. The ionic radius of Sn^{4+} (0.69 Å) is similar to that of Ga^{3+} (0.62 Å), providing greater lattice stability compared to Si dopants (0.40 Å). Moreover, Sn acts as a deep donor, effectively reducing self-compensation effects and improving doping efficiency. This leads to enhanced carrier transport and improved device performance by mitigating unintentional defect states that can degrade conductivity.[8,9]

Despite its promising properties, a major challenge in β-Ga_2O_3-based devices is their inherently low thermal conductivity (11–27 W/m K), which can limit high-power operation efficiency.[10,11] To mitigate this limitation, integrating β-Ga_2O_3 with silicon carbide (SiC), which has a significantly higher thermal conductivity (347 W/m K) and a small lattice mismatch (1.3%), offers

an effective solution. Ga_2O_3/SiC heterostructures, such as Schottky diodes, can not only improve thermal management but also leverage SiC's superior electron mobility for better high-frequency performance.[12]

In this study, Sn-doped β-Ga_2O_3/SiC hetero-structured Schottky diodes were fabricated using Mist-chemical vapor deposition Mist-CVD, with varying [Sn]/[Ga] ratios of 0%, 3%, 5%, and 10% to systematically investigate the impact of Sn incorporation. The J–V characteristics revealed that the Ga_2O_3 film with a 3% [Sn]/[Ga] ratio exhibited the highest conductivity, lowest specific on-resistance ($R_{on,sp}$), and minimal leakage current. X-ray photoelectron spectroscopy (XPS) confirmed that Sn atoms were substitutionally incorporated into the β-Ga_2O_3 lattice, effectively modifying its electronic properties. Furthermore, deep-level transient spectroscopy (DLTS) analysis indicated that the trap states associated with gallium vacancies (V_{Ga}) and carbon vacancies (V_C), which were prominent in undoped films ([Sn]/[Ga] = 0%), disappeared upon Sn doping. These findings demonstrate a viable approach for optimizing Sn-doped Ga_2O_3/SiC hetero-structured Schottky barrier diodes with reduced defect densities and enhanced electrical performance.

II. EXPERIMENTAL

An n-type SiC epitaxial layer (doping concentration: 1.0×10^{16} cm^{-3}, thickness: 7 μm) was grown on a highly doped 4H-SiC substrate (1.0×10^{19} cm^{-3}) through hydride vapor phase epitaxy (HVPE). The Ga_2O_3 epilayer deposited by Mist-CVD had a thickness of approximately 1 μm. Prior to deposition, the substrate surface was cleaned using standard cleaning and dilute hydrofluoric acid (DHF) treatment. For ohmic contact, 150 nm of nickel (Ni) was created on the back side of the SiC substrate by electron-beam (E-beam) evaporation and rapid thermal annealing (RTA) at 1050 °C for 1 min. The Sn-doped β-Ga_2O_3 epilayers were deposited using Mist-CVD, as illustrated in Fig. 1(a). For deposition, a precursor solution of 0.025 mol/l gallium (III) acetylacetonate $Ga(C_5H_7O_2)_3$ (with 99.99% purity) in acidic water (pH = 1) and 0%, 3%, 5%, 10% variation in the [Sn]/[Ga] ratio were employed. For Sn incorporation, a tin mist precursor was co-introduced in the same acidic aqueous medium; the nominal solution [Sn]/[Ga] ratios were 0%, 3%, 5%, and 10%. No evaporation of a volatile Sn compound was used. The growth temperature of the β-Ga_2O_3 films was fixed at 900 °C for 2 h. Then, the Ni Schottky contact (thickness: 70 nm, diameter: 1000 μm) was formed on the β-Ga_2O_3 epi-layer using E-beam evaporation. Figure 1(b) shows the device structure of the fabricated Ga_2O_3/SiC hetero-structured Schottky barrier diode. Figure 1(c) presents the band alignment of the Ga_2O_3/4H-SiC heterojunction, where the conduction band offset and valence band offset are estimated to be ~0.76 and ~1.34 eV, respectively. This staggered band configuration significantly affects carrier transport and defect states at the interface, forming the basis for the DLTS analysis of SiC-related defects such as the $Z_{1/2}$ center.

III. RESULTS AND DISCUSSION

Figure 2(a) J–V characteristics of Ga_2O_3/4H-SiC hetero-structured Schottky diodes with [Sn]/[Ga] ratio variations of 0%, 3%, 5%, and 10% in the room temperature. The Sn-doped diode demonstrated a higher on-state current density level compared to the undoped diode. Each diode exhibits a low leakage current of less than 1×10^{-11} A/cm^2. The Ga_2O_3/SiC heterojunction diode with 3% [Sn]/[Ga] ratio shows the lowest leakage current of

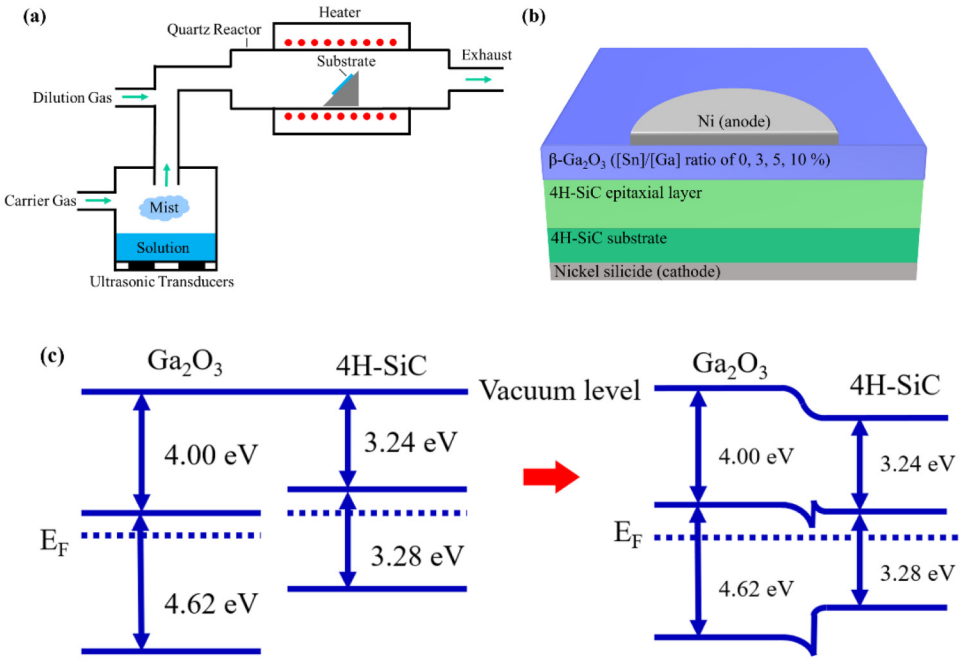

FIG. 1. (a) Schematic drawing of the Mist-CVD system. (b) Device structure of fabricated Ga_2O_3/SiC hetero-structured Schottky barrier diodes. (c) Band alignment diagram of the Ga_2O_3/4H-SiC heterojunction, illustrating conduction and valence band offsets.

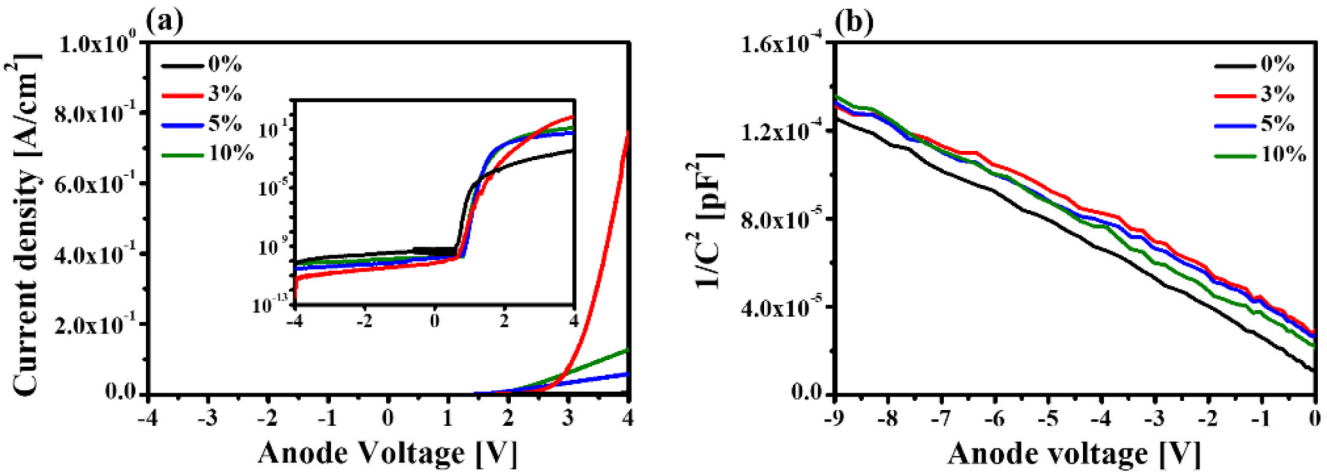

FIG. 2. (a) Linear and log scale(inset) plot of current density vs anode voltage characteristics of Ga_2O_3/4H-SiC hetero-structured Schottky diodes with [Sn]/[Ga] ratio variations of 0%, 3%, 5%, and 10%. (b) $1/C^2$ vs reverse voltage bias applied to Ga_2O_3/4H-SiC hetero-structured Schottky diodes with [Sn]/[Ga] ratios of 0%, 3%, 5%, and 10% at a frequency of 50 kHz.

1.51×10^{-12} A/cm^2 and $R_{on,sp}$ of 0.61 Ω cm^2. The on/off ratio improved 1.66×10^5 times as measured at −4 and 4 V. The barrier height (Φ_B) of the diodes was determined from the ln(J)–V characteristics based on the thermal emission (TE) model,[13]

$$\varnothing_B = \frac{kT}{q} \ln \frac{AA^* T^2}{I_s}.$$

In the above equation, k represents the Boltzmann constant, q is the electron charge, T denotes the temperature, I_s refers to the saturation current, while A is the contact area. The term A^* represents the Richardson constant, which is 41 A/cm^2 K^2 with the effective electron mass of β-Ga_2O_3: $m^*_e = 0.34\ m_0$.[14]

Figure 2(b) shows the $1/C^2$–V plot measured at a bias of −9 ∼ 0 V and frequency of 50 kHz. The donor doping concentrations (N_d) were extracted from the $1/C^2$–V plot by using the following equation:

$$N_d(W) = \frac{2}{q\varepsilon_S\varepsilon_0 A^2} \left[\frac{1}{\delta(1/C^2)/\delta V}\right],$$

$$W = \sqrt{\frac{2\varepsilon_s(V_{bi} + V_R)}{qN_d}}.$$

The donor state density, $N_d(W)$, depends on the depletion width and can be determined from the slope of the linear region in the plot. From the slope of the $1/C^2$–V characteristics, the donor concentration of the Sn-doped Ga_2O_3/SiC heterostructured Schottky diodes was determined to be approximately 2×10^{16} cm^{-3}. Furthermore, the built-in voltage (V_{bi}) is obtained by identifying the X-axis intercept of the extrapolated straight line. The structural parameters derived from the J–V and $1/C^2$–V characteristics are summarized in Table I.

Figure 3 presents the XPS spectra near the Sn 3d peak for each Ga_2O_3/SiC heterostructured Schottky barrier diode with different [Sn]/[Ga] ratios. As the [Sn]/[Ga] ratio increased, the intensity of the Sn $3d_{3/2}$ and Sn $3d_{5/2}$ peaks also increased, confirming the successful incorporation of Sn atoms as substitutional dopants in the β-Ga_2O_3 lattice.[15] In the Sn–O binary system, SnO and SnO_2 are the only thermodynamically stable phases.[16,17] The XPS spectra revealed two distinct Sn 3d components, corresponding to Sn^{4+} and Sn^{2+}

TABLE I. Parameters derived from J–V, $1/C^2$–V characteristics.

[Sn]/[Ga] ratio	0%	3%	5%	10%
On/off ratio	6.20×10^6	1.03×10^{11}	1.87×10^8	2.02×10^8
Leakage current (A/cm^2)	1.11×10^{-10}	1.51×10^{-12}	3.03×10^{-11}	7.11×10^{-11}
$R_{on,sp}$ (Ω cm^2)	2.51	0.61	1.72	1.33
Φ_B (eV)	0.98	1.10	1.02	0.99
V_{bi} (V)	0.61	1.54	1.45	1.15
Doping concentration (cm^{-3})	8.1×10^{15}	2.1×10^{16}	2.2×10^{16}	2.4×10^{16}
Depletion width (μm)	1.15	0.75	0.73	0.68

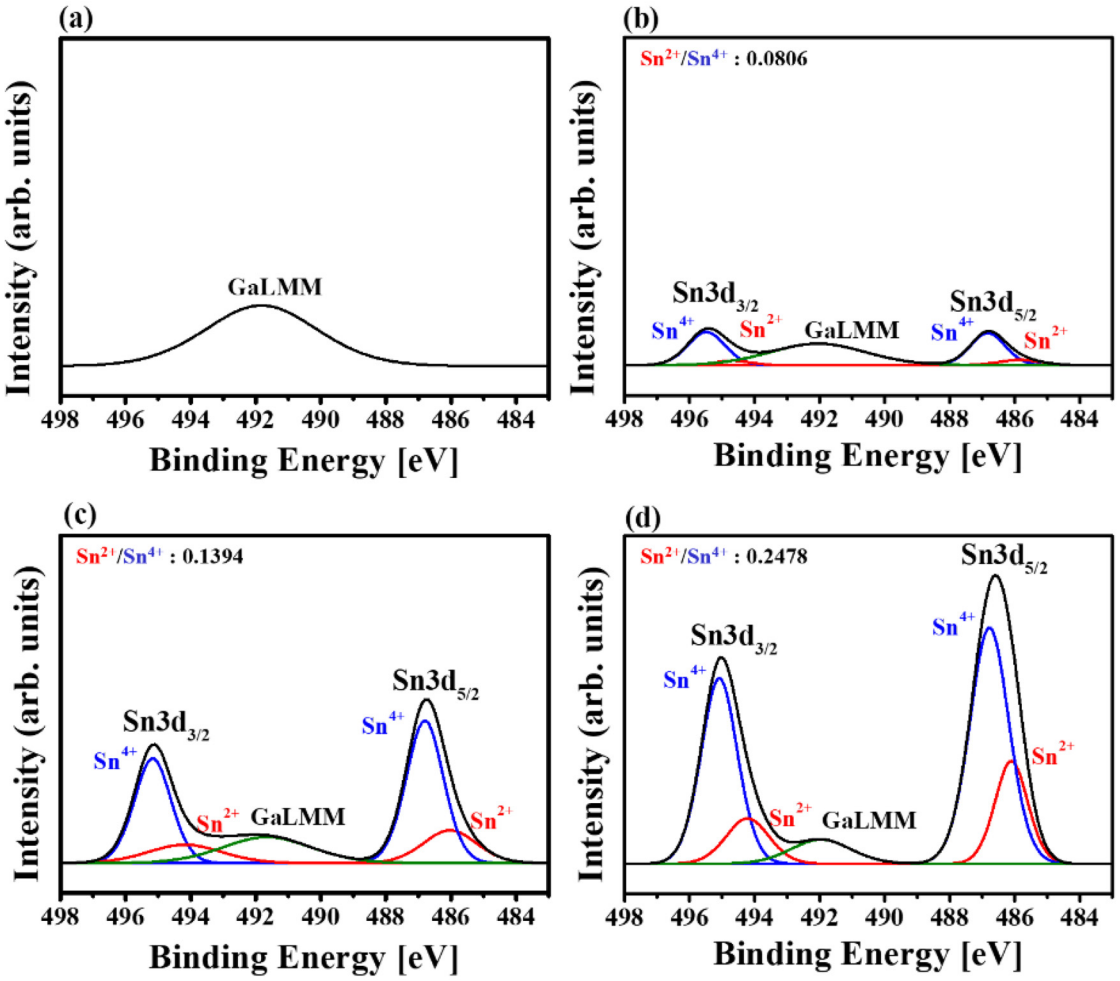

FIG. 3. XPS spectra of Ga_2O_3/SiC hetero-structured Schottky barrier diodes with [Sn]/[Ga] ratios of (a) 0%, (b) 3%, (c) 5%, and (d) 10%.

oxidation states, with an average peak separation of 0.7 eV.[18] The dominance of Sn^{4+} signals over Sn^{2+} suggests that Sn preferentially forms SnO_2, which has a lower Gibbs free energy of formation compared to SnO.[19] As the [Sn]/[Ga] ratio increased, the Sn^{2+}/Sn^{4+} area ratio continued to rise, suggesting that the formation of SnO became more favorable at higher Sn concentrations.[20] This trend suggests that excessive Sn incorporation promotes a shift in the oxidation state equilibrium, potentially modifying the local chemical environment and influencing the electronic structure of β-Ga_2O_3.

Figure 4(a) presents the DLTS spectra of Ga_2O_3/SiC hetero-structured Schottky barrier diodes with [Sn]/[Ga] ratios of 0%, 3%, 5%, 10% and SiC epi layer. In the DLTS measurements, we used the reverse bias $V_r = -9$ V, pulse voltage $V_p = 0.5$ V, and filling-pulse width = 5 ms, and rate window = 8.9×10^{-2} s ($t_1 = 1.09 \times 10^{-2}$ s, $t_2 = 9.99 \times 10^{-2}$ s) with 200 cycles per temperature to improve signal-to-noise. Three peaks (A1, A2, A3) were detected at a [Sn]/[Ga] ratio of 0%, but in Sn-doped Ga_2O_3/SiC heterojunction diodes with [Sn]/[Ga] ratios of 3%, 5%, and 10%, these peaks disappeared, and new peaks emerged near 380 and 480 K. From DLTS spectra, we calculated the trap density of each trap with the following equation :

$$n_t = 2N_d \frac{\Delta C}{C_r \left\{ \frac{W_r^2}{\left((W_r - \lambda)^2 - (W_0 - \lambda)^2\right)} \right\}},$$

where ΔC represents the change in capacitance, C_r is the reverse capacitance, and N_d is the net carrier concentration, and W_r, W_0 is the depletion widths at reverse bias and during the filling pulse, respectively.[21,22]

Fig. 4(a) shows the Arrhenius plot of each defect in Ga_2O_3/SiC hetero-structured Schottky barrier diodes with

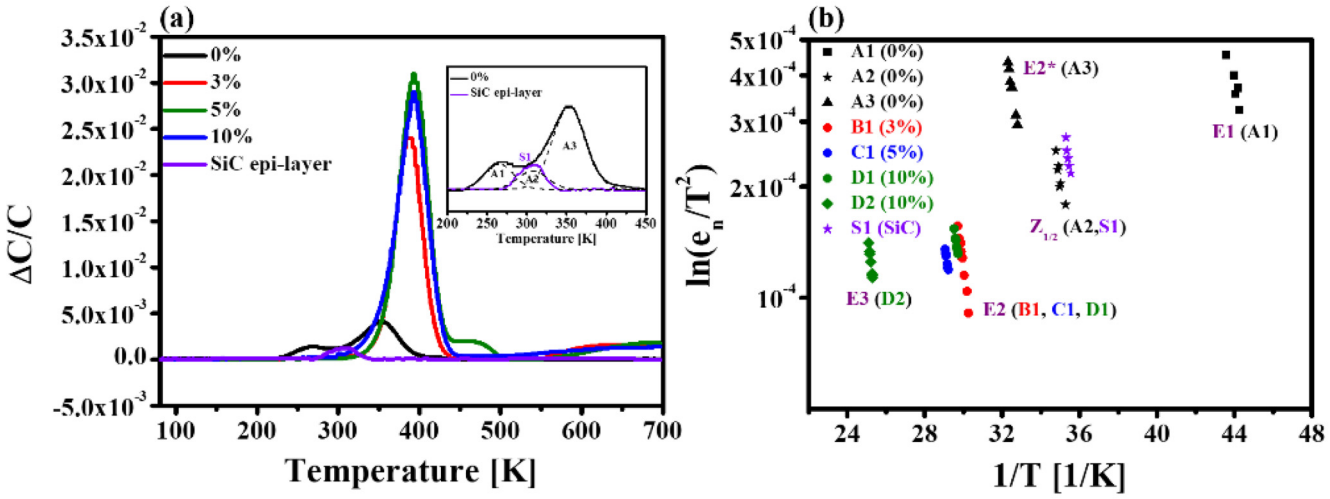

FIG. 4. (a) DLTS spectra, and (b) Arrhenius plot of Ga_2O_3/SiC hetero-structured Schottky barrier diodes with [Sn]/[Ga] ratios of 0%, 3%, 5%, 10% and SiC-epi layer (without Ga_2O_3 deposition).

[Sn]/[Ga] ratios of 0%, 3%, 5%, and 10%. Capture cross section and activation energy were calculated by the following equation, using the Arrhenius plot,[23,24]

$$e_n = \sigma_n \beta T^2 \exp\left(-\frac{E_c - E_t}{kT}\right),$$

$$ln\left[\frac{e_n}{T^2}\right] = \ln(\beta\sigma_n) - \frac{E_c - E_t}{kT}.$$

Here, β accounts for temperature-independent factors (e.g., the effective mass). The activation energy (ΔE) is obtained from the slope of the Arrhenius plot, and the capture cross section (σ_n) from the intercept of the extrapolated line at $1/T = 0$. Activation energies are reported within the employed temperature windows. A rigorous enthalpy–entropy separation typically requires expanded window coverage and bias-dependent controls in heterojunction DLTS and was not the focus of the present study. Detailed trap parameters are summarized in Table II. Under our bias and filling-pulse conditions, the depletion region weights traps within the near-interface portion of the Ga_2O_3/SiC junction; the probed Ga_2O_3 depth is approximately 0.9 μm. The window reported in the main text is representative of spectral display; the Arrhenius plots were constructed from emission rates extracted by time-domain fits to the transients acquired at each temperature under the same pulsing conditions.

Based on the calculated trap parameters, the possible origins of each trap were estimated. Three defects (A1, A2, and A3) were detected at a [Sn]/[Ga] ratio of 0%, corresponding to the defect from impurities, the $Z_{1/2}$ defect from carbon vacancies (V_C), and the E2* defect from gallium vacancies (V_{Ga}) and V_{Ga}–V_O divacancy-related candidate, consistent with recent assignments.[25–31] Among these defects, $Z_{1/2}$ is known as a carrier lifetime killer defect in SiC.[29,30] To directly verify this assignment, we additionally performed DLTS on a bare n-type 4H-SiC epitaxial layer without Ga_2O_3 deposition. The dominant level in the epi-only control appears near 0.62 eV, which closely matches the A2 peak observed in the [Sn]/[Ga] ratio of 0% device, supporting our identification of A2 as the $Z_{1/2}$ center in 4H-SiC. Under our DLTS bias condition, the space-charge region in the undoped device extends through the 1 μm Ga_2O_3 layer and reaches 4H-SiC (reach-through);

TABLE II. Trap parameters derived from DLTS analysis.

[Sn]/[Ga] ratio	0%			3%	5%	10%		SiC epi
Labels	A1	A2	A3	B1	C1	D1	D2	S1
Activation energy (E_C–E_T) (eV)	0.594	0.621	0.758	0.818	0.825	0.827	1.107	0.625
Capture cross section (σ_n) (cm^2)	6.3×10^{-14}	3.0×10^{-16}	1.3×10^{-14}	3.2×10^{-14}	3.1×10^{-15}	1.6×10^{-15}	5.1×10^{-14}	3.3×10^{-16}
Trap density (n_T) (cm^{-3})	4.8×10^{13}	4.3×10^{13}	1.4×10^{14}	7.7×10^{14}	1.1×10^{15}	3.7×10^{15}	5.7×10^{13}	5.1×10^{13}
Possible attributions	Impurities	V_C	V_{Ga}, V_{Ga}–V_O	Sn_{Ga}, Fe-related	Sn_{Ga}, Fe-related	Sn_{Ga}, Fe-related	V_O, Ti donor	V_C

therefore, the SiC-related center ($Z_{1/2}$) is effectively sensed. As DLTS measurement analyzes the trap parameters by measuring the capacitance transient of the device, the SiC-related defects can be detected near the Ga_2O_3/SiC interface. The E2* defect, associated with V_{Ga}, critically affects the electrical characteristics of Ga_2O_3.[27,28] V_{Ga} can degrade the stability of Ga_2O_3 under high temperature or stress conditions by capturing electrons and acting as trap sites, functioning as compensating centers that reduce the free electron concentration.

In Sn-doped diodes ([Sn]/[Ga] ratio of 3%, 5%, and 10%), the E2 defect and E3 defect caused by Sn_{Ga} and oxygen vacancy (V_O) were detected. The $E_c-0.82$ eV level is also consistent with Fe-related acceptor behavior widely reported for the E2 center; we, therefore, list it as a candidate Fe-related level.[32] It is well known that Sn generally behaves as a shallow donor in β-Ga_2O_3, with possible DX-like behavior depending on the occupied lattice site.[8,9,31,33] As [Sn]/[Ga] increases, Sn_{Ga} related traps have increased, and V_{Ga}-related traps reduced by Sn occupied vacancy sites. Under our DLTS conditions, the depletion width does not exceed the 1 μm Ga_2O_3 layer, and the $Z_{1/2}$ center is not detected within our measurement sensitivity. In the Ga_2O_3/SiC diode with a [Sn]/[Ga] ratio of 10%, E3 defects, which are noted as candidate Ti donors in an ingrown material or V_O-related when introduced by irradiation, were detected.[31,34] Sn substitutes on the Ga site (Sn^{4+}) and modifies the local bonding network, increasing the fraction of Sn–O bonds and potentially facilitating V_O formation, which can reduce carrier lifetime and increase leakage current.[35,36] Although oxygen vacancies may increase trap-assisted leakage current, they can also enhance n-type conductivity by providing shallow donor levels. This may explain why the sample with [Sn]/[Ga] = 10% showed slightly higher conductivity than the 5% sample, despite the increased trap density. As shown in XPS data, the rise in the Sn^{2+}/Sn^{4+} area ratio indicates that SnO formation becomes more favorable. This process suggests a reduction in local oxygen availability, which could be linked to the creation of oxygen vacancies, further aligning with the increased presence of SnO.

IV. CONCLUSION

We investigated the electrical and defect properties of Ga_2O_3/SiC heterojunction diodes fabricated using mist-CVD by varying the [Sn]/[Ga] ratio. The diodes with a [Sn]/[Ga] ratio of 3% exhibited the highest on/off ratio, lowest $R_{on,sp}$, and minimal leakage current, indicating optimized charge transport properties. XPS analysis revealed that the signal at a binding energy of 485 eV could be deconvoluted into two peaks at approximately 487 and 485.2 eV, corresponding to Sn^{4+} and Sn^{2+} oxidation states, respectively. The dominance of the Sn^{4+} state suggests that Sn preferentially forms SnO_2 due to its lower Gibbs free energy of formation compared to SnO. However, as the Sn concentration increased, the Sn^{2+}/Sn^{4+} area ratio continued to rise, indicating that higher Sn incorporation promotes SnO formation. This shift suggests a modification in the oxidation state equilibrium, which may influence the local electronic environment. The reduction of gallium vacancy-related traps (V_{Ga}), attributed to Sn occupying V_{Ga} sites, led to improved carrier mobility, enhanced electrical conductivity, and overall device performance. However, at higher Sn concentrations, the formation of oxygen vacancy (V_O) defects was observed, which can degrade carrier lifetime and increase leakage current, highlighting a trade-off between enhanced doping and defect generation. The integration of Sn-doped Ga_2O_3 with SiC presents a promising approach for high-power and high-frequency applications. The reduction of deep-level defects, particularly, V_{Ga} and $Z_{1/2}$ related states, suggests improved carrier transport characteristics. Additionally, the high thermal conductivity of SiC allows for enhanced heat dissipation, addressing one of the key limitations of Ga_2O_3-based devices. These findings indicate that optimized Sn doping could enhance both the thermal stability and RF performance of Ga_2O_3/SiC-based devices.

ACKNOWLEDGMENTS

This research was conducted by the Research Grant of Kwangwoon University in 2024 and the Korea Evaluation Institute of Industrial Technology (Nos. RS-2022-00144027 and RS-2022-00154720).

AUTHOR DECLARATIONS

Conflict of Interest

The authors have no conflicts to disclose.

Author Contributions

Tae-Hee Lee: Conceptualization (equal); Data curation (equal); Formal analysis (equal); Investigation (equal); Methodology (equal); Validation (equal); Visualization (equal); Writing – original draft (equal); Writing – review & editing (equal). **Ji-Soo Choi:** Formal analysis (supporting); Investigation (supporting). **Se-Rim Park:** Data curation (equal); Methodology (equal). **Seung-Hwan Chung:** Validation (supporting); Visualization (supporting). **Geon-Hee Lee:** Data curation (supporting); Formal analysis (supporting). **Jae Hyeok Lim:** Methodology (supporting); Resources (supporting). **Si-Young Bae:** Methodology (supporting); Resources (supporting); Writing – review & editing (supporting). **Sang-Mo Koo:** Funding acquisition (equal); Supervision (equal); Writing – review & editing (equal).

DATA AVAILABILITY

The data that support the findings of this study are available from the corresponding author upon reasonable request.

REFERENCES

[1]A. R. Balog, C. Lee, D. Duarte-Ruiz, S. V. Gayathri Ayyagari, J. Jesenovec, A. E. Chmielewski, L. Miao, B. L. Dutton, J. McCloy, C. Cocchi, E. Ertekin, and N. Alem, "Determination of the β to γ phase transformation mechanism in Sc-and Al-alloyed β-Ga_2O_3 crystals," ACS Appl. Electron. Mater. **6**(10), 7095–7105 (2024).

[2]J. D. Blevins, K. Stevens, A. Lindsey, G. Foundos, and L. Sande, "Development of large diameter semi-insulating gallium oxide (Ga_2O_3) substrates," IEEE Trans. Semicond. Manuf. **32**(4), 466–472 (2019).

[3]M. H. Wong, O. Bierwagen, R. J. Kaplar, and H. Umezawa, "Ultrawide-bandgap semiconductors: An overview," J. Mater. Res. **36**(23), 4601–4615 (2021).

[4]X. Q. Zheng, H. Zhao, and P. X. L. Feng, "A perspective on β-Ga2O3 micro/nanoelectromechanical systems," Appl. Phys. Lett. **120**(4), 040502 (2022).
[5]J. Montes, C. Kopas, H. Chen, X. Huang, T. H. Yang, K. Fu, and Y. Zhao, "Deep level transient spectroscopy investigation of ultra-wide bandgap (201) and (001) β-Ga_2O_3," J. Appl. Phys. **128**(20), 205701 (2020).
[6]A. Y. Polyakov, N. B. Smirnov, I. V. Shchemerov, E. B. Yakimov, S. J. Pearton, C. Fares, J. Yang, F. Ren, J. Kim, P. B. Lagov, V. S. Stolbunov, and A. Kochkova, "Defects responsible for charge carrier removal and correlation with deep level introduction in irradiated β-Ga_2O_3," Appl. Phys. Lett. **113**(9), 092102 (2018).
[7]Z. Wang, X. Chen, F. F. Ren, S. Gu, and J. Ye, "Deep-level defects in gallium oxide," J. Phys. D: Appl. Phys. **54**(4), 043002 (2021).
[8]M. H. Wong and M. Higashiwaki, "Vertical β-Ga_2O_3 power transistors: A review," IEEE Trans. Electron Devices **67**(10), 3925–3937 (2020).
[9]X. Zhou, Q. Liu, G. Xu, K. Zhou, X. Xiang, Q. He, W. Hao, G. Jian, X. Zhao, and S. Long, "Realizing high-performance β-Ga_2O_3 MOSFET by using variation of lateral doping: A TCAD study," IEEE Trans. Electron Devices **68**(4), 1501–1506 (2021).
[10]M. Labed, N. Sengouga, C. Venkata Prasad, M. Henini, and Y. S. Rim, "On the nature of majority and minority traps in β-Ga_2O_3: A review," Mater. Today Phys. **36**, 101155 (2023).
[11]W. Xu, T. You, Y. Wang, Z. Shen, K. Liu, L. Zhang, H. Sun, R. Qian, Z. An, F. Mu, T. Suga, G. Han, X. Ou, Y. Hao, and X. Wang, "Efficient thermal dissipation in wafer-scale heterogeneous integration of single-crystalline β-Ga_2O_3 thin film on SiC," Fund. Res. **1**(6), 691–696 (2021).
[12]M. E. Liao, K. Huynh, Z. Cheng, J. Shi, S. Graham, and M. S. Goorsky, "Thermal transport and structural improvements due to annealing of wafer bonded β-Ga_2O_3|4H-SiC," J. Vac. Sci. Technol. A **41**(6), 063203 (2023).
[13]G. Wang and Y. Zhou, "Thermal management modeling for β-Ga_2O_3-highly thermal conductive substrates heterostructures," IEEE Trans. Compon. Packag. Manuf. Technol. **12**(4), 638–646 (2022).
[14]H. He, R. Orlando, M. A. Blanco, R. Pandey, E. Amzallag, I. Baraille, and M. Rérat, "First-principles study of the structural, electronic, and optical properties of Ga_2O_3 in its monoclinic and hexagonal phases," Phys. Rev. B **74**(19), 195123 (2006).
[15]X. Zhang, H. Lee, J. Kim, E. J. Kim, and J. Park, Materials **11**, 46 (2018).
[16]S. Cahen, N. David, J. M. Fiorani, A. Maı^tre, and M. Vilasi, Thermochim. Acta **403**, 275 (2003).
[17]P. A. Wright, *Extractive Metallurgy of Tin* (Elsevier Scientific Pub. Co., Amsterdam, 1982).
[18]J. M. Themlin, M. Chtaïb, L. Henrard, P. Lambin, J. Darville, and J. M. Gilles, Phys. Rev. B **46**, 2460 (1992).
[19]M. Kanayama, T. Oku, T. Akiyama, Y. Kanamori, S. Seo, J. Takami, Y. Ohnishi, Y. Ohtani, and M. Murozono, Energy Power Eng. **05**, 18 (2013).
[20]H. Ryou *et al.*, "Hydrothermal synthesis and photocatalytic property of Sn-doped β-Ga_2O_3 nanostructure.," ECS J. Solid State Sci. Technol. **9**(4), 045009 (2020).
[21]C. Van Opdorp, "Evaluation of doping profiles from capacitance measurements," Solid-State Electron. **11**(4), 397–406 (1968).
[22]P. Blood and J. W. Orton, "The electrical characterization of semiconductors: Majority carriers and electron states," Tech. Phys. **14**, i–xxiii (1992).
[23]D. V. Lang, "Deep-level transient spectroscopy: A new method to characterize traps in semiconductors," J. Appl. Phys. **45**(7), 3023–3032 (1974).
[24]N. M. Johnson, "Measurement of semiconductor–insulator interface states by constant-capacitance deep-level transient spectroscopy," J. Vac. Sci. Technol. **21**(2), 303–314 (1982).
[25]Z. P. Wang, N. Sun, X. X. Yu, H. H. Gong, X. L. Ji, F. F. Ren, S. L. Gu, Y. D. Zheng, R. Zhang, A. Y. Kuznetsov, and J. D. Ye, "Performance limiting inhomogeneities of defect states in ampere-class Ga_2O_3 power diodes," Appl. Phys. Rev. **11**(2), 021413 (2024).
[26]M. Fregolent, F. Piva, M. Buffolo, C. De Santi, A. Cester, M. Higashiwaki, G. Meneghesso, E. Zanoni, and M. Meneghini, "Advanced defect spectroscopy in wide bandgap semicondutors: Review and recent results," J. Phys. D: Appl. Phys. **57**, 433002 (2024).
[27]N. Manikanthababu, H. Sheoran, P. Siddham, and R. Singh, "Review of radiation-induced effects on β-Ga_2O_3 materials and devices," Crystals **12**(7), 1009 (2022).
[28]A. Y. Polyakov *et al.*, "Deep level defect states in β-, α-, and ε-Ga_2O_3 crystals and films: Impact on device performance.," J. Vac. Sci. Technol. A **40**(2), 020804 (2022).
[29]K. Kawahara, X. Thang Trinh, N. Tien Son, E. Janzén, J. Suda, and T. Kimoto, "Investigation on origin of Z 1/2 center in SiC by deep level transient spectroscopy and electron paramagnetic resonance," Appl. Phys. Lett. **102**(11), 112106 (2013).
[30]S. Sasaki, K. Kawahara, G. Feng, G. Alfieri, and T. Kimoto, "Major deep levels with the same microstructures observed in n-type 4H–SiC and 6H–SiC," J. Appl. Phys. **109**(1), 013705 (2011).
[31]A. Langørgen, L. Vines, and Y. Kalmann Frodason, "Perspective on electrically active defects in β-Ga_2O_3," J. Appl. Phys. **135**, 195702 (2024).
[32]A. A. Vasilev, A. I. Kochkova, A. Y. Polyakov, A. A. Romanov, N. R. Matros, L. A. Alexanyan, I. V. Shchemerov, and S. J. Pearton, "Observation of temperature-dependent capture cross section for main deep-levels in β-Ga_2O_3," J. Appl. Phys. **136**, 025701 (2024).
[33]Y. K. Frodason *et al.*, "Diffusion of Sn donors in β-Ga_2O_3," APL Mater. **11**(4), 041121 (2023).
[34]A. Y. Polyakov *et al.*, "Impact of irradiation on deep centers in β-Ga_2O_3" (2024).
[35]Y. Shen, H.-P. Ma, L. Gu, J. Zhang, W. Huang, J.-T. Zhu, and Q.-C. Zhang, "Atomic-level Sn doping effect in Ga_2O_3 films using plasma-enhanced atomic layer deposition," Nanomaterials **12**, 4256 (2022).
[36]S. C. Siah, R. E. Brandt, K. Lim, L. T. Schelhas, R. Jaramillo, M. D. Heinemann, D. Chua, J. Wright, J. D. Perkins, C. U. Segre, R. G. Gordon, M. F. Toney, and T. Buonassisi, "Dopant activation in Sn-doped Ga_2O_3 investigated by x-ray absorption spectroscopy," Appl. Phys. Lett. **107**, 252103 (2015).